Frequency-Dependent OPFET Characteristics with Improved Absorption under Back Illumination

Nandita Saha Roy and B. B. Pal

***Abstract*—A simple analytical model of an ion-implanted GaAs metal–semiconductor–field-effect transistor (MESFET) is useful for computer aided design of GaAs devices and integrated circuits (IC's) and device parameter acquisition. The present paper aims at presenting a frequency dependent analytical model of GaAs optically illuminated field-effect transistor (OPFET) with improved absorption under back illumination. Instead of the conventional front illumination through the source, gate and drain we consider the incident radiation to enter the device through the substrate. Two cases are considered: one in which the fiber is inserted partially into the substrate and the other, in which the fiber is inserted upto the active layer—substrate interface. The later case represents improved absorption in the active layer of the device. The current-voltage characteristics and the transconductance of the device for different signal modulated frequencies have been evaluated. The frequency dependence of internal and external photovoltages and the photocurrent have also been calculated and discussed. The results indicate significant improvement over published data using front illumination.**

***Index Terms*—AC model, GaAs optically illuminated field-effect transistor (OPFET), optically controlled metal–semiconductor–field-effect transistor (MESFET) photonic devices.**

I. Introduction

THE rapid development of GaAs technology requires the development of an accurate and simple device model of GaAs metal–semiconductor–field-effect transistor (MESFET). The optical control of such a device provides an added advantage of obtaining electrical isolation and immunity from electromagnetic interference.

In recent years, considerable attention has been given to GaAs optically illuminated field-effect transistors (OPFET's) for their charming applications in optically controlled amplifiers and oscillators. Some authors [1], [2] have also reported high speed optical detection with GaAs MESFET's. Experimental investigation of microwave characteristics of GaAs MESFET under optically direct-controlled conditions was carried out by Mizuno [3]. At about the same time, de Salles [4] carried out theoretical and experimental characterization of GaAs OPFET with emphasis on photovoltaic effects. An analytical ac model of a GaAs OPFET considering the effects of radiation and surface recombination was developed by Mishra *et al.* [5]. Using the same structure, Zebda *et al.*[6] analyzed the effect of carrier concentration on the lifetime of minority carriers under time varying conditions. These theoretical models provided a simple and accurate closed form expressions for the device characteristics in terms of physical parameters and are important in giving a physical insight into the device operation.

With the increasing use of optical transmissions in different systems, development of device structure with improved coupling efficiency between optical and microwave energies have become very important. For optimum optical/microwave interaction, optical absorption in the active region of the device is to be improved. In the present model, we consider a cavity in the substrate of an ion-implanted GaAs MESFET where the fiber is inserted and the optical radiation is allowed to fall on the device from the substrate side. Two cases are of interest—one in which the fiber is inserted partially into the substrate and the radiation enters the device through the substrate and the other in which fiber is inserted upto the active layer-substrate junction so that strong absorption occurs in the active layer of the OPFET. The fundamental physical mechanism behind optical illumination is the absorption of photons in the valence band of the material thereby creating electrons and holes. The photogenerated electrons contribute to the drain-source current when a drain-source voltage is applied and the holes develop a photovoltage at the schottky junction and the p-n junction of the device resulting in the modulation of the channel conductance. The variation of the ac component of the drain current, photovoltages, transconductance and gain with signal modulated frequency and radiation flux density have been studied and compared with published results under front illumination. The theory is presented below:

II. Theory

The schematic structure of the ion-implanted GaAs OPFET with back illumination is shown in Fig. 1(a) and (b) for the two cases. In Fig. 1(a), the fiber is inserted partially into the substrate so that the absorption takes place in both substrate and active region. In Fig. 1(b), the fiber is inserted upto the junction of the substrate and the active layer where photoabsorption takes place in the active region only. The drain-source current flows along the x-direction and the illumination is incident along the y-direction of the device. Electron-hole pairs are generated due to absorption of photons in the neutral substrate region, the active layer-substrate depletion region, the neutral channel region and the schottky junction depletion region. The optically generated electrons move toward the channel and contribute to the drain-source current when a drain-source voltage is applied while the holes move in the opposite direction. When these holes cross the junction a photovoltage is developed. This voltage being forward biased reduces the depletion width of both the junctions. For the first case where the substrate effect is included, an external photovoltage (V_{op1}) is developed across

Manuscript received April 27, 1999; revised November 16, 1999.

The authors are with the Department of Electronics Engineering, Institute of Technology, Banaras Hindu University, Varanasi 221005, India.

Publisher Item Identifier S 0733-8724(00)02193-9.

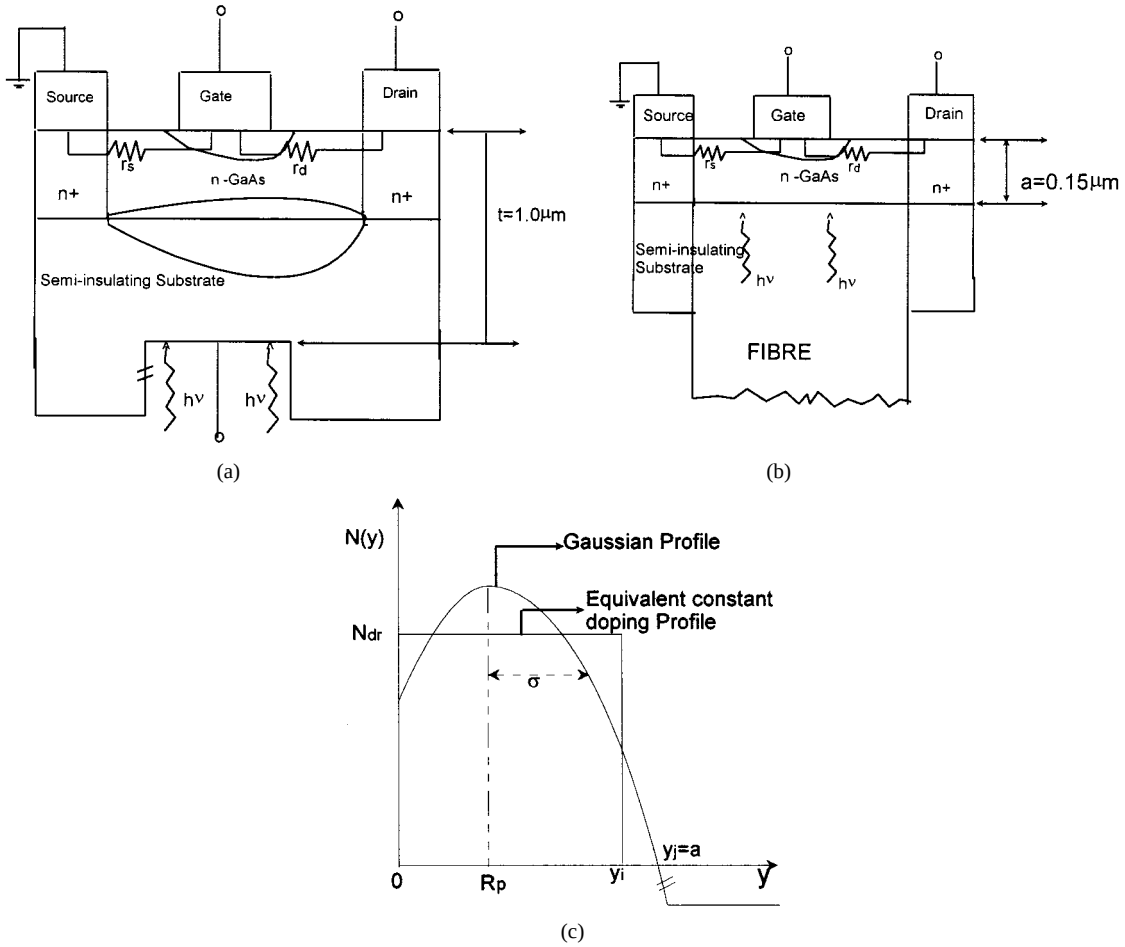

Fig. 1. (a) Schematic structure of the device with fiber inserted partially into the substrate. (b) Schematic structure of the device when the fiber is inserted up to the substrate-active layer interface. (c) Gaussian profile and its equivalent constant doping distribution of impurities in the active layer.

the schottky junction and an internal photovoltage (V_{op2}) is daveloped across the substrate-active layer junction. For the second case where no substrate effect is involved the only photovoltage developed is the external photovoltage V_{op1} across the schottky junction.

The device consists of a p-type uniformly doped semi-insulating substrate followed by an epitaxially grown ion-implanted active layer of n-type doping. The ion-implanted profile is represented by the Gaussian distribution given by [7]

$$N(y) = \frac{Q}{\sigma\sqrt{2\pi}} \exp\left[-\left(\frac{y - R_p}{\sigma\sqrt{2}}\right)^2\right] \tag{1}$$

where Q is the implanted dose, σ is the straggle parameter and R_p is the projected range.

Under dark condition the drain current is contributed by the majority carriers (electrons) contributed by the impurity atoms in the channel. Under illumination the photogenerated electrons and holes in the substrate and channel neutral and depletion regions are obtained by solving the respective continuity equations [8]. The time-dependent continuity equations for electrons and holes are represented in one dimension as

$$\frac{\partial n(y,t)}{\partial t} = \frac{1}{q}\frac{\partial J_n(y,t)}{\partial y} + G - \frac{n(y,t)}{\tau_n} - \frac{R_s \tau_n}{S_n} \tag{2}$$

for electrons and

$$\frac{\partial p(y,t)}{\partial t} = -\frac{1}{q}\frac{\partial J_p(y,t)}{\partial y} + G - \frac{p(y,t)}{\tau_p} - \frac{R_s \tau_p}{S_p} \tag{3}$$

for holes.

G is the volume generation rate of carriers and is assumed to vary exponentially with distance. Taking the surface as the reference since the radiation is incident from the surface side, G follows the following relation:

$$G = \alpha\phi e^{-\alpha(t-y)} \tag{4}$$

where t is the surface to substrate thickness, α is the absorption coefficient per unit length and ϕ is the radiation flux density per unit area per second.

J_n and J_p are the electron and hole current densities given by

$$J_n = q v_y n + q D_n \frac{dn}{dy} \tag{5}$$

$$J_p = q v_y p - q D_p \frac{dp}{dy} \tag{6}$$

In the above equations different terms have their usual meaning as in [5]. The term R_s in (2) and (3) is calculated using the relation [5]

$$R_s = \frac{N_T k_n k_p (n_s p_s - n_t p_t)}{k_n (n_s + n_t) + k_p (p_s + p_t)} \tag{7}$$

where $n_s = \alpha\phi\tau_n$ and $p_s = \alpha\phi\tau_p$, and other terms have the same meaning as in [5]. S_n and S_p in (2) and (3) are the surface recombination velocities for electrons and holes, respectively. In the above expressions, we consider both surface recombination due to trap centres at or close to the surface and bulk recombination. The recombination due to traps at the interface of the active layer-substrate region has however been neglected.

The incident radiation is assumed to be modulated by a signal of frequency ω. Thus under small signal condition

$$\phi = \phi_0 + \phi_1 e^{j\omega t} \tag{8.a}$$
$$n = n_0 + n_1 e^{j\omega t} \tag{8.b}$$
$$p = p_0 + p_1 e^{j\omega t} \tag{8.c}$$
$$G = G_0 + G_1 e^{j\omega t} \tag{8.d}$$

where "zero" indicates the dc value and "one" indicates the ac value.

Assuming that only negative trap centers are present and that the traps close to the surface are important, (6) may be approximated as

$$R_s \approx N_t k_p p_s$$

or

$$R_s = (N_T k_p \alpha\phi_0\tau_p) + (N_T k_p \alpha\tau_p\phi_1 e^{j\omega t}) \tag{9}$$

where

$$k_n n_s \gg k_p p_s \quad \text{and} \quad n_s p_s \gg n_t p_t.$$

By combining (2)–(5), (7), and (8) we obtain two sets of differential equations under ac and dc conditions.

A. Calculation of Photovoltage

The photovoltage is developed due to flow of holes across the junctions. The transport mechanism of carriers in the depletion region is due to drift and recombination. Thus the continuity equation for holes is represented by the first-order differential equation as

$$\frac{\partial p}{\partial t} = -\frac{\partial p}{y} - \frac{p}{v_y\tau_p} + \frac{\alpha\phi}{v_y} e^{-\alpha(t-y)} - \frac{R_s\tau_p}{S_p v_y}. \tag{10}$$

Under back illumination, carrier generation is maximum at the substrate end at $y = t$ and $y = 0$ refers to the surface of the device where generation is minimum. This is evident from (4) for generation rate. So the constant associated with the exponentially decreasing function with y is assumed zero from physical condition. The ac solution for the hole density is obtained as

$$p(y) = \frac{\alpha\phi_1\tau_{\omega p}}{(1 + \alpha v_y \tau_{\omega p})} e^{-\alpha(t-y)} - \frac{N_T k_p \tau_p \tau_{\omega p} \phi_1 \alpha}{S_p} \tag{11}$$

where $(1/\tau_{\omega p}) = (1/\tau_p) + j\omega$, $\tau_{\omega p}$ is the life time of holes under ac condition. $\tau_{\omega p}$ is independent of ω if $1/\tau_p \gg \omega$.

Using (11), the number of holes crossing the junction at $y = a$ is calculated. The internal photovoltage $V_{\text{op}2}$ across the channel substrate junction is obtained using the relation

$$V_{\text{op}2} = \frac{kT}{q} \ln\left(\frac{J_p(a)}{J_{s2}}\right) = \frac{kT}{q} \ln\left(\frac{q v_y p(a)}{J_{s2}}\right) \tag{12}$$

where J_{s2} is the saturation current density for the p-n junction. The surface recombination is zero for $V_{\text{op}2}$.

The external photovoltage $V_{\text{op}1}$ across the schottky junction is calculated using the relation

$$V_{\text{op}1} = \frac{kT}{q} \ln\left(\frac{J_p}{J_s}\right) = \frac{kT}{q} \ln\left(\frac{q v_y p(0)}{J_{s1}}\right) \tag{13}$$

where J_{s1} is the reverse saturation current density across the Schottky junction [9]. $p(0)$ is the number of holes crossing the junction at $y = 0$ and is also calculated from (11).

Equations (12) and (13) represent the ac photovoltages.The importance of calculating $V_{\text{op}1}$ and $V_{\text{op}2}$ lies in the fact that they modify the depletion widths of both Schottky junction and n-p junction considerably. y_{dg}, the extension of the schottky junction depletion region in the channel measured from the surface is expressed as,

$$y_{\text{dg}} = \left[\frac{2\varepsilon}{qN_{\text{dr}}}(\phi_B - \Delta + v(x) - v_{\text{gs}})\right]^{\frac{1}{2}} \tag{14}$$

assuming the abrupt junction approximation where N_{dr} is the equivalent constant doping concentration of ion-implanted profile (Fig. 1(c)). Under illumination y_{dg} is modified to

$$y'_{\text{dg}} = \left[\frac{2\varepsilon}{qN_{\text{dr}}}(\phi_B - \Delta + v(x) - v_{\text{gs}} - v_{\text{op}1})\right]^{\frac{1}{2}}. \tag{15}$$

Similarly, the extension of the n-p junction depletion region in the channel measured from the surface y_{ds} also gets modified to y'_{ds} under illumination. y_{ds} is written as (assuming abrupt junction approximation)

$$y_{\text{ds}} = a - \frac{N_A}{N_{\text{dr}}}\left[\frac{2\varepsilon}{qN_A}(v_{\text{bi}} + v(x) - v_{\text{bs}})\right]^{\frac{1}{2}}. \tag{16}$$

under dark and modified to

$$y'_{\text{ds}} = a - \frac{N_A}{N_{\text{dr}}}\left[\frac{2\varepsilon}{qN_A}(v_{\text{bi}} + v(x) - v_{\text{bs}} - v_{\text{op}2})\right]^{\frac{1}{2}} \tag{17}$$

under illumination.

In the above equations N_{dr} is calculated using the relation [see Fig. 1(c)]

$$N_{\text{dr}} y_i = \int_0^{yj} \frac{Q}{\sigma\sqrt{2\pi}} \exp\left[-\left(\frac{y - R_p}{\sigma\sqrt{2}}\right)^2\right] dy \tag{18}$$

where y_i is the distance for which $N_{\text{dr}} y_i$ is same as that of implanted charge in the channel and y_j is the junction depth of the active region from the surface which is same as "a," the active layer thickness.

B. Calculation of the AC Drain-Source Current

The ac component of the total drain-source current is contributed by the carriers due to ion-implantation and optical generation in the channel and substrate regions. It can be represented as,

$$I_{\rm ds}(\text{total}) = I_{\rm ion} + I_{\rm ch} + I_{\rm dep} + I_{\rm sub}. \tag{19}$$

When the substrate is not involved as in the second case mentioned earlier, the contribution is due to ion-implantation and photogeneration in the neutral channel region and gate depletion region.

In this calculation, we follow the model similar to that for high pinch off MESFET devices [9]. The procedure followed is given below. The drain-source current is expressed as

$$I_{\rm ds} = I_{\rm sat}(1+\lambda V_i)\tanh \eta V_i \tag{20}$$

where

$$V_i(\text{the input voltage}) = V_{\rm ds} - I_{\rm sat}(r_s + r_d) \tag{21a}$$

$$\eta = \frac{G_{\rm ch}}{I_{\rm sat}}; \quad G_{\rm ch} \text{ being the channel conductance} \tag{21b}$$

$$\lambda = 0.025 \text{ (constant)}$$

where r_s and r_d are the source and drain resistances, respectively.

The saturation current is defined as

$$I_{\rm sat} = I_{\rm total}\left[K - (K^2 - 1 + U_{\rm gs})^{\frac{1}{2}}\right] \tag{22}$$

where

$$K = 1 + \left(\frac{r_s I_{\rm total}}{2V_{\rm po}}\right)$$

and

$$U_{\rm gs} = \frac{V_{\rm bi} - V_{\rm gs}}{V_{\rm po}}$$

$I_{\rm total}$ is the channel current and is determined from gradual channel approximation.

i) The ac drain-source current due to ion-implantation is obtained using the relation

$$I_{\rm ds} = \frac{\mu Z}{L}\int_0^{v_{\rm ds}} Q_{\rm ion}\, dv \tag{23}$$

where $Q_{\rm ion}$ is the ac channel charge due to ion-implantation and is calculated from

$$Q_{\rm ion} = q\int_{y'_{\rm dg}}^{y'_{\rm ds}} N(y)\, dy \tag{24}$$

Z is the channel width and L is the channel length. The frequency dependence of the ion-implanted current arises due to the frequency variation of the photovoltages. Under dark condition when the photovoltages are zero, we obtain the dc value of the drain-source current due to ion-implantation.

The contribution to the drain-source current $(I_{\rm ds})$ due to ion-implantation is obtained as

$$I_{\rm ion} = \frac{q\mu Z Q}{2L}[I_2 - I_1] \tag{25}$$

where I_1 and I_2 are given in the Appendix.

ii) AC current due to carriers generated in the neutral region: When the frequency modulated optical signal is incident on the device, the number of generated electrons are obtained by solving (2). Since the transport mechanism in the neutral region is diffusion and recombination in absence of any drain-source voltage the continuity equation is a second order differential equation.

The frequency dependent ac equation is given by

$$\frac{d^2 n_1}{dy^2} - \frac{n_1}{D_n \tau_{\omega n}} = -\frac{\alpha\phi_1 e^{-\alpha y}}{D_n} \tag{26}$$

in which $(1/\tau_{\omega n}) = (1/\tau_n) + j\omega$. $\tau_{\omega n}$ is the life time of electrons under ac condition. $\tau_{\omega n}$ is independent of ω if $(1/\tau_n) \gg \omega$.

The effect of surface recombination is not present in case of electrons since only the presence of negative traps has been assumed at or close to the surface. The solution to the above equation for the neutral channel region is obtained as

$$n_1 = \alpha\phi_1\tau_{\omega n}\left[1 + \frac{1}{(\alpha^2 L_{n\omega}^2 - 1)}\right]\exp(-\alpha(t - y_{\rm dg})) \times \exp\left[-\left(\frac{y_{\rm dg} - y}{L_{n\omega}}\right)\right] - \frac{\alpha\phi_1\tau_{\omega n}e^{-\alpha(t-y)}}{(\alpha^2 L_{n\omega}^2 - 1)} \tag{27}$$

where the boundary condition applied is: at $y = y_{\rm dg}$ $n = \alpha\phi\tau_{\omega n}e^{-\alpha(t-y_{\rm dg})}$.

In the above equation, $L_{n\omega} = \sqrt{D_n\tau_{\omega n}}$ and is called the frequency dependent diffusion length or ac diffusion length of electrons. In the above equation one of the constants is assumed zero from physical conditions since the carriers generated reduce with distance y. The ac charge density developed due to the electrons generated in the neutral channel region is given by

$$Q_{\rm ch} = q\int_{y_{\rm ds}}^{y_{\rm ds}} n_1\, dy.$$

So, the ac drain-source current contributed by photogenerated electrons in the channel neutral region is calculated as

$$I_{\rm ch} = \frac{\mu Z}{L}\int_0^{v_{\rm ds}} Q_{\rm ch}\, dv = \frac{q\mu Z}{L}\left[\alpha\phi_1 L_{n\omega}\left\{\tau_{\omega n} + \frac{1}{A}\right\}(e^{-\alpha t}I_4 - I_3) + \frac{\phi_1}{A}(I_5 - I_3)\right] \tag{28}$$

where I_3, I_4 and I_5 are given in the Appendix and

$$A = D_n\left(\alpha - \frac{1}{L_{n\omega}^2}\right).$$

For the first case where the fiber is inserted partially into the substrate the generation in the substrate neutral region

TABLE I
VALUES OF DIFFERENT PARAMETERS
ASSUMED FOR CALCULATION

Values of different parameters assumed for calculation

Parameter	Name	Value	Unit
σ	Straggle Parameter	0.383×10^{-7}	(m)
R_p	Projected Range	0.861×10^{-7}	(m)
μ_n	Electron Mobility	0.45	(m^2/V.s)
μ_p	Hole Mobility	0.04	(m^2/V.s)
Z	Channel Width	100×10^{-6}	(m)
α	Absorption Coefficient	1.0×10^{6}	(m^{-1})
τ_n	Electron Lifetime	1.0×10^{-6}	(s)
τ_p	Hole Lifetime	1.0×10^{-8}	(s)
v_y	Carrier velocity in y-direction	1.2×10^{5}	(m/s)
t	Thickness of the MESFET including substrate	1.0×10^{-6}	(m)
L	Channel Length	3.0×10^{-6}	(m)
a	active layer thickness	0.15×10^{-6}	(m)
Δ	Position of fermi level below the conduction band	0.02	(ev)
ϕ_B	Schottky barrier height	0.9	(ev)
ε_0	Permittivity	1.04335×10^{-10}	(F/m)
N_t	Trap density	1.0×10^{15}	(m^{-2})
k_p	Capture factors for holes	3.1×10^{-17}	(m^3/s)
k_n	Capture factors for electrons	3.1×10^{-15}	(m^3/s)
v_p	Pinch-off voltage	1.68	V
v_{bs}	Substrate Potential	0.0	V
N_A	Substrate doping conc.	1.0×10^{20}	m^{-3}
N_{dr}	Equivalent const.doping conc.	0.658×10^{23}	m^{-3}

also contribute to the drain-source current. So under that condition (25) is solved by applying the boundary condition, at

$$y = t, \quad n = \alpha\phi\tau_{\omega n}$$

The number of generated carriers (n_2) in the neutral substrate region is obtained as

$$n_2 = \alpha\phi_1\tau_{\omega n}\left[1 + \frac{1}{(L_{n\omega}^2\alpha^2 - 1)}\right] \times \exp\left(-\frac{(t-y)}{L_{n\omega}}\right) - \frac{\alpha\phi_1 e^{-\alpha(t-y)}}{(L_{n\omega}^2\alpha^2 - 1)}. \quad (29)$$

The contribution to the total ac channel current from the neutral substrate region is given by

$$I_{\text{sub}} = \frac{\mu Z}{L}\int_0^{v_{\text{ds}}} Q_{\text{sub}}\, dv$$

$$I_{\text{sub}} = \frac{q\mu Z}{L}\left[\alpha\phi_1 L_{n\omega}\left\{\tau_{\omega n} + \frac{1}{A}\right\}(v_{\text{ds}} - I_6) + \frac{\phi_1\alpha}{A}(v_{\text{ds}} - I_7)\right] \quad (30)$$

where I_6 and I_7 are given in the Appendix and Q_{sub} is defined as

$$Q_{\text{sub}} = q\int_{y_w}^{y_t} n_2\, dy$$

y_w is the extension of the channel-substrate depletion region in the substrate measured from the surface given by,

$$y_w = y_{\text{ds}} + \left[\frac{2\varepsilon}{qN}(v_{\text{bi}} + v_{\text{ds}} - v_{\text{bs}})\right]^{\frac{1}{2}} \quad (31)$$

where

$$\left(\frac{1}{N}\right) = \left(\frac{1}{N_A}\right) + \left(\frac{1}{N_{\text{dr}}}\right)$$

iii) AC current due to carriers generated in the depletion regions:
The transport mechanism in the depletion region is due to drift and recombination. So the frequency dependent continuity equation is of the form

$$\frac{\partial n}{\partial y} - \frac{n\tau_{\omega n}}{v_y} + \frac{\alpha\phi_1}{v_y}e^{-\alpha(t-y)} = 0 \quad (32)$$

where the constant associated with the exponentially decreasing function of y is assumed zero from physical condition.
The solution of the above equation gives the number of generated electrons in the depletion region and is written as

$$n_3 = \frac{\alpha\phi_1\tau_{\omega n}}{(1 - \alpha v_y\tau_{\omega n})}e^{-\alpha(t-y)} \quad (33)$$

As mentioned in Fig. 1(a) and (b) there are two different depletion regions in the device and have been considered separately.

a) Depletion region below the gate: The contribution to the total ac channel current due to generation in the gate depletion region is calculated as

$$I_{\text{dep1}} = \frac{\mu Z}{L}\int_0^{v_{\text{ds}}} Q_{\text{dep1}}\, dv$$

where

$$Q_{\text{dep1}} = q\int_0^{y_{\text{dg}}} n_3\, dy$$

Hence

$$I_{\text{dep1}} = \frac{\phi_1\tau_{\omega n}}{(1 - \alpha v_y\tau_{\omega n})}I_8 + \frac{\phi_1\tau_{\omega n}}{(1 - \alpha v_y\tau_{\omega n})}V_{\text{ds}} \quad (34)$$

b) Depletion region at the active layer-substrate interface: The charge developed due to electrons generated in this region is given by

$$Q_{\text{dep2}} = q\int_{y_{\text{ds}}}^{y_w} n_3\, dy$$

So the AC current is obtained as

$$I_{\text{dep2}} = \frac{\mu Z}{L}\int_0^{v_{\text{ds}}} Q_{\text{dep2}}\,dv = \frac{q\mu Z}{L}\left[\frac{\phi_1\tau_{\omega n}}{(1-\alpha v_y\tau_{\omega n})}(I_9 - I_{10})\right] \tag{35}$$

where I_8, I_9 and I_{10} in (33) and (34) are given in the Appendix.

Summation of (29), (31), (34), and (35) gives the total ac channel current from which the total ac drain-source current is calculated using the relation (19).

C. Calculation of AC Transconductance

The ac transconductance of the device is evaluated using the relation

$$g_m = \left[\frac{dI_{\text{ds}}}{dV_{\text{gs}}}\right]_{V_{\text{ds}}\,constant} \tag{36}$$

III. Results and Discussions

Numerical calculations have been carried out for the drain-source current, the photogenerated current and the transconductance of the device under ac condition. The device parameters and the values of different constants have been listed in the table.

Fig. 2(a) and (b) shows the plots of the external and the internal ac photovoltages against signal frequency at different radiation flux densities. Both the external photovoltage (v_{op1}) and internal photovoltage (v_{op2}) remain constant upto 100 GHz after which the value decreases with increasing frequency. This is because the coefficient associated with the exponential term in (11) contributes significantly at a frequency above 100 GHz. The recombination term has very little contribution. The variations of photovoltages are similar to that reported earlier [10]. Comparison of Fig. 2(a) and 2(b) shows that for a particular frequency and flux density V_{op2} is larger than V_{op1}. This is because the saturation current density for p-n junction is less compared to that of schottky junction. Moreover, under back illumination the number of carriers generated at the active layer-substrate depletion region is more than that in the gate depletion region.

The ac component of the drain-source current (I_{ds}) has been plotted against drain-source voltage of the device at different signal frequencies and is shown in Fig. 3. The figure also represents the two cases mentioned earlier. I_{ds} is observed to decrease with the increase in frequency at a particular drain-source voltage. Further, when the radiation is incident at the active layer-substrate interface (case 2) there is enhanced absorption in the active region. So a larger I_{ds} is obtained compared to the case where a finite substrate effect is involved (case 1).

Fig. 4 represents a comparison of I–V characteristics of the present model with that of Mishra *et al.* [5] and Zebda *et al.* [6] for the same device structure. At a frequency of 0.1 GHz and flux density of $10^{21}/\text{m}^2\cdot\text{s}$, the present model shows higher current compared to [5] and [6] because in [5] and [6] the channel width modulation due to photovoltage has not been considered. Further, the models considered illumination incident on the semitransparent gate of the device.

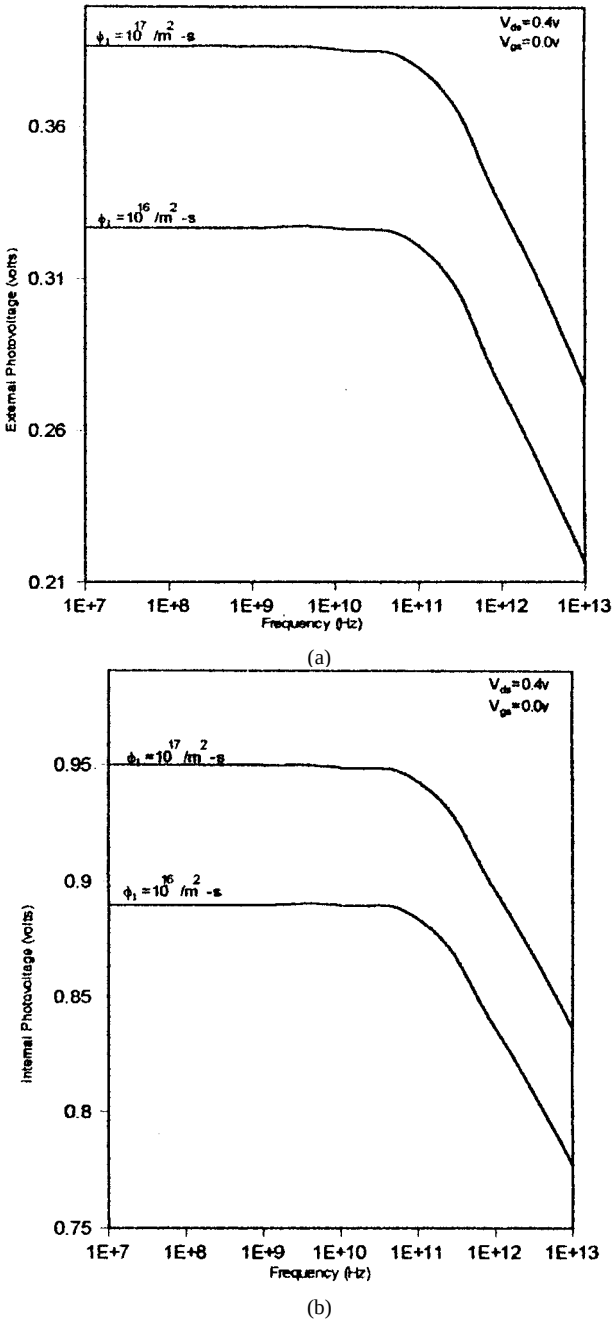

Fig. 2. (a) Variation of external photovoltage with frequency under different flux densities. (b) Variation of internal photovoltage with frequency under different incident flux densities.

The plot of ac drain-source current against frequency and flux density are shown in Fig. 5(a) and (b), respectively, for different conditions of incident radiation and the device structure. For varying flux density of incident illumination, I_{ds} (ac part) remains constant upto 1 MHz after which it decreases with the increase in frequency. This is because the effect of frequency becomes important when $(1/\tau_n) \leq \omega$.The changes of I_{ds} with frequency is similar to that in [10]. I_{ds} is higher for case 2 than case 1. From Fig. 5(b) it is observed that at a flux density above $10^{17}/\text{m}^2$-s, the effect of illumination on I_{ds} is significant below

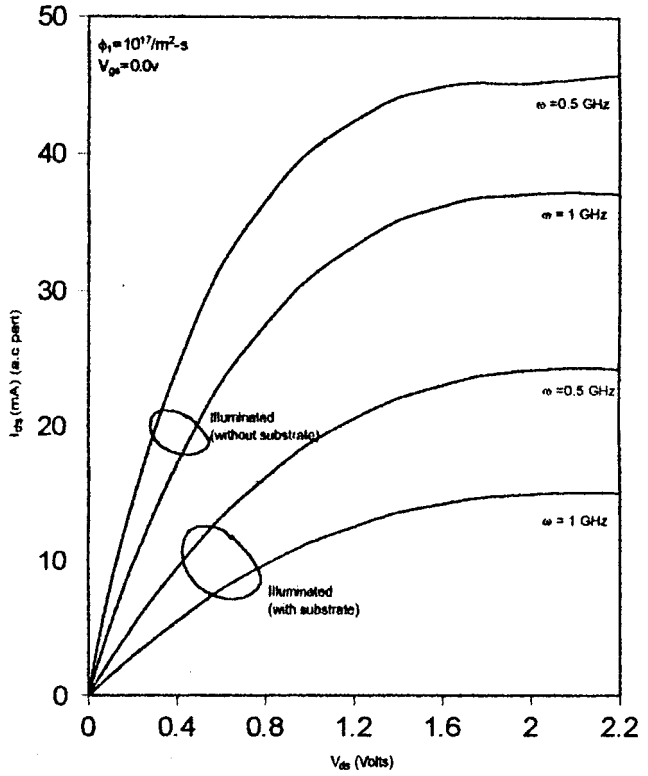

Fig. 3. I–V Characteristics of the device for different signal frequencies.

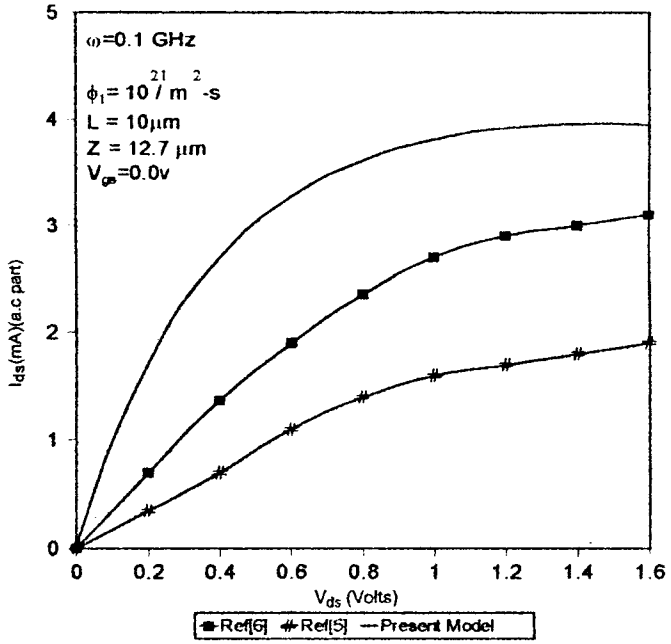

Fig. 4. Comparison of I–V Characteristics of the present model with those of Refs. [5] and ref [6].

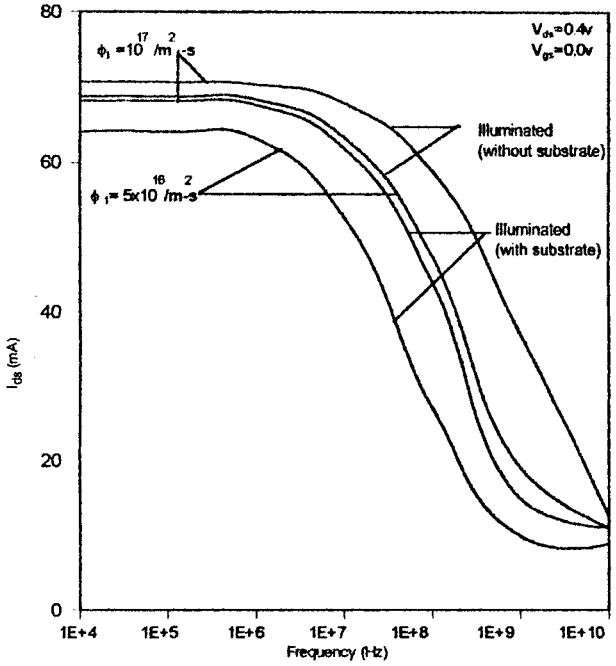

Fig. 5. (a) Drain-source current (ac part) against frequency for varying flux densities. (b) Drain-source current (ac part) against flux density for different frequencies and drain-source voltages.

which the effect is negligible. At lower frequency $I_{\rm ds}$ is larger at a particular incident flux density. Both the plots show the effect of two different drain-source voltages also. Increase in $V_{\rm ds}$ increases $I_{\rm ds}$ at a constant frequency and flux density.

Fig. 6 shows the plot of the I–V characteristics of the device for varying active layer thickness for the two cases and at a particular frequency. At 1 GHz, it is observed that the increase in the active layer thickness increases the value of $I_{\rm ds}$ at a constant $V_{\rm ds}$ and flux density.

Fig. 7 represents the variation of the ac transconductance of the device with $V_{\rm gs}$ for the two cases—with and without substrate effect under back illumination. The transconductance is an important device parameter which determines the maximum cut-off frequency of operation of the device. At a particular value of $V_{\rm gs}$, the transconductance is lower for higher frequency. The transconductance increases gradually as one goes from depletion mode (normally-ON) to enhancement

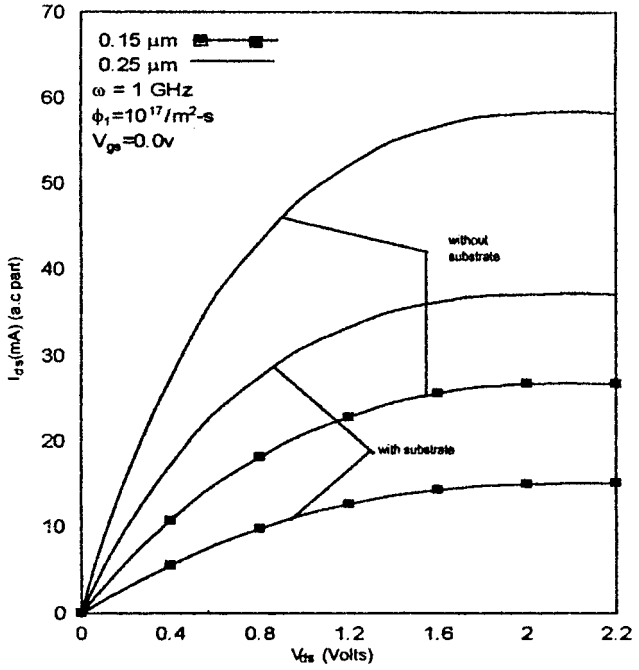

Fig. 6. Variation of drain-source current (ac part) with drain-source voltage for different active layer thickness.

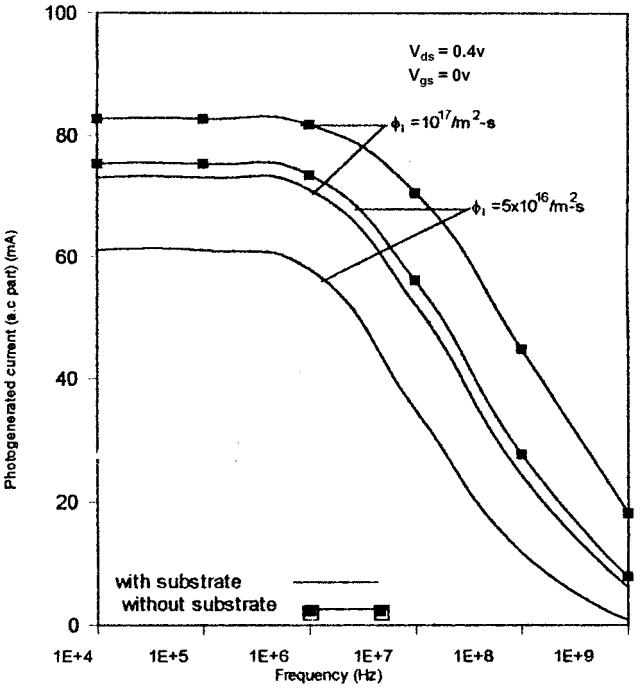

Fig. 8. Photogenerated current against frequency at different flux densities of incident radiation.

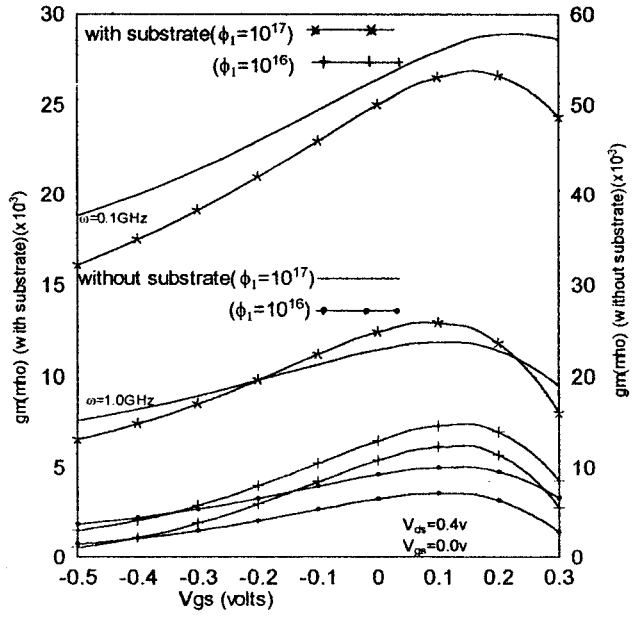

Fig. 7. Transconductance versus gate-source voltage for different frequencies.

mode (normally-OFF). However when the gate voltage is larger than 0.1 V, g_m reaches a peak and then decreases steadily with the gate voltage as the gate voltage becomes more and more positive. It is because at higher positive gate voltages some of the electrons are attracted toward the gate instead of reaching the drain. Also the holes which where crossing the Schottky junction gets repelled and $V_{\rm opl}$ decreases. So the cumulative effect of the above two phenomena causes the decrease in the transconductance. With the increase in the flux density the transconductance increases indicating that optical illumination controls the device performance.

The plot of ac photogenerated current with frequency is shown in Fig. 8. The photogenerated current is taken as the current due to generated carriers as a result of photoabsorption. Increase in the flux density increases the generation of electron-hole pairs and the photogenerated current. The photogenerated current remains constant upto 1 MHz after which it decreases with the increase in frequency.

However, in these calculations we have not considered any reflection from the surfaces which will slightly reduce the drain current and transconductance of the device.

IV. Conclusion

A new model for the OPFET frequency dependent characteristics have been outlined under back illumination with and without substrate effect. The significant feature of this new analytical model is the higher drain-source current of the device due to improved absorption. Internal photovoltaic effect is found to be more significant than the external photovoltage. The comparison of the device characteristics with and without substrate effect shows that the photogeneration in the active layer is significant due to enhanced absorption in the active region when no substrate effect is present and enhance the photogenerated current considerably. The increase in the active layer thickness also increases the drain current. The present OPFET model with back illumination may be considered to be an useful method for the design of a highly sensitive optical transducer, detector, preamplfier and radio frequency optical switch in communication and computers.

APPENDIX

The drain-source current due to ion-implanted profile is given by (25) in which the terms I_1 and I_2 are defined as

$$I_1 = \int_0^{V_{\rm ds}} \operatorname{erf}\left(\frac{y_{\rm dg}-R_p}{\sigma\sqrt{2}}\right) dv$$
$$I_2 = \int_0^{V_{\rm ds}} \operatorname{erf}\left(\frac{y_{\rm ds}-R_p}{\sigma\sqrt{2}}\right) dv.$$

They are evaluated as

$$I_1 = \frac{2\sigma^2 qN_{\rm dr}}{\varepsilon}\left[\frac{a_2}{2}\left\{-a_2\operatorname{erf}a_2 - \frac{1}{\sqrt{\pi}}\left(e^{-a_2^2}-1\right)\right\} + \frac{a_2'}{2}\left\{a_2'\operatorname{erf}a_2' + \frac{1}{\sqrt{\pi}}\left(e^{-a_2'^2}-1\right)\right\} + \frac{1}{4}\{\operatorname{erf}a_2 - \operatorname{erf}a_2'\} + \frac{1}{2\sqrt{\pi}}(a_2'-a_2)\right]$$

$$I_2 = \frac{q\sigma\sqrt{2}N_{\rm dr}^2}{\varepsilon N_A}\left[(R_p-a)\left\{-a_3\operatorname{erf}a_3 - \frac{1}{\sqrt{\pi}}\left(e^{-a_3^2}-1\right) + a_3'\operatorname{erf}a_3' + \frac{1}{\sqrt{\pi}}\left(e^{-a_3'^2}-1\right)\right\} + \sigma\sqrt{2}\left\{\frac{a_3'}{2}\left(a_3'\operatorname{erf}a_3' + \frac{e^{-a_3'^2}}{\sqrt{\pi}}\right) - \frac{a_3}{2}\left(a_3\operatorname{erf}a_3 + \frac{e^{-a_3^2}}{\sqrt{\pi}}\right) - \frac{1}{4}(\operatorname{erf}a_3' - \operatorname{erf}a_3) + \frac{1}{\sqrt{\pi}}(a_3'-a_3)\right\}\right].$$

In the above expressions

$$a_2 = \frac{[y_{\rm dg}]_{V(x)=0}-R_p}{\sigma\sqrt{2}} \quad a_3 = \frac{[y_{\rm ds}]_{V(x)=0}-R_p}{\sigma\sqrt{2}}$$
$$a_2' = \frac{[y_{\rm dg}]_{V(x)=V_{\rm ds}}-R_p}{\sigma\sqrt{2}} \quad a_3' = \frac{[y_{\rm ds}]_{V(x)=V_{\rm ds}}-R_p}{\sigma\sqrt{2}}.$$

In (28), the drain-source current due to photogenerated electrons in the neutral channel region has the terms I_3, I_4, and I_5. They are expressed as

$$I_3 = \frac{qN_{\rm dr}}{\varepsilon}\left[\frac{k_2}{\alpha}\exp\{-\alpha(t-k_2)\} - \frac{1}{\alpha^2}\exp\{-\alpha(t-k_2)\} - \frac{k_1}{\alpha}\exp\{-\alpha(t-k_1)\} + \frac{1}{\alpha^2}\exp\{-\alpha(t-k_1)\}\right]$$

$$I_4 = \frac{qN_{\rm dr}}{\varepsilon\left(\alpha-\frac{1}{L_{n\omega}}\right)^2}\left[\left\{\left(\alpha-\frac{1}{L_{n\omega}}\right)k_2-1\right\}\exp\left(\frac{m_2}{L_{n\omega}}\right)\times\exp\left[\left(\alpha-\frac{1}{L_{n\omega}}\right)k_2\right] - \left\{\left(\alpha-\frac{1}{L_{n\omega}}\right)k_1-1\right\}\times\exp\left(\frac{m_1}{L_{n\omega}}\right)\exp\left[\left(\alpha-\frac{1}{L_{n\omega}}\right)k_1\right]\right]$$
$$- \frac{qN_A}{\varepsilon\left(\alpha-\frac{1}{L_{n\omega}}\right)^2 L_{n\omega}}\left[\left(\left\{\left(\alpha-\frac{1}{L_{n\omega}}\right)k_2-1\right\}\times\frac{\exp\left(\frac{m_2}{L_{n\omega}}\right)}{(m_2-a)}\left[\frac{k_2\exp\left(\alpha-\frac{1}{L_{n\omega}}\right)k_2}{\left(\alpha-\frac{1}{L_{n\omega}}\right)} - \frac{2\exp\left(\alpha-\frac{1}{L_{n\omega}}\right)k_2}{\left(\alpha-\frac{1}{L_{n\omega}}\right)^3}\left\{\left(\alpha-\frac{1}{L_{n\omega}}\right)k_2-1\right\}\right]\right)\right.$$
$$\left. - \left(\left\{\left(\alpha-\frac{1}{L_{n\omega}}\right)k_1-1\right\}\frac{\exp\left(\frac{m_1}{L_{n\omega}}\right)}{(m_1-a)}\times\left[\frac{k_1\exp\left(\alpha-\frac{1}{L_{n\omega}}\right)k_1}{\left(\alpha-\frac{1}{L_{n\omega}}\right)} - \frac{2\exp\left(\alpha-\frac{1}{L_{n\omega}}\right)k_1}{\left(\alpha-\frac{1}{L_{n\omega}}\right)^3}\times\left\{\left(\alpha-\frac{1}{L_{n\omega}}\right)k_1-1\right\}\right]\right)\right]$$

$$I_5 = \frac{qN_{\rm dr}^2}{\varepsilon N_A}\left[\frac{m_2}{\alpha}\exp[-\alpha(t-m_2)] - \frac{1}{\alpha^2}\exp[-\alpha(t-m_2)] - \frac{a}{\alpha}\exp[-\alpha(t-m_2)] - \frac{m_1}{\alpha}\exp[-\alpha(t-m_1)] + \frac{1}{\alpha^2}\exp[-\alpha(t-m_1)] + \frac{a}{\alpha}\exp[-\alpha(t-m_1)]\right]$$

where

$$k_1 = y_{\rm dg}]_{V(x)=0} \quad m_1 = y_{\rm ds}]_{V(x)=0}$$
$$k_2 = y_{\rm dg}]_{V(x)=V_{\rm ds}} \quad m_1 = y_{\rm ds}]_{V(x)=V_{\rm ds}}$$

The terms I_6 and I_7 of (30) has been evaluated to be

$$I_6 = \frac{qN_A}{N'^2}\left[(y_w|_{v=v_{\rm ds}}-a)L_{n\omega}\exp\left(\frac{t-y_w|_{v=v_{\rm ds}}}{L_{n\omega}}\right) - L_{n\omega}^2\exp\left(\frac{t-y_w|_{v=v_{\rm ds}}}{L_{n\omega}}\right) + (y_w|_{v=0}-a)L_{n\omega}\times\exp\left(\frac{t-y_w|_{v=0}}{L_{n\omega}}\right) - L_{n\omega}^2\exp\left(\frac{t-y_w|_{v=v_{\rm ds}}}{L_{n\omega}}\right)\right]$$

and

$$I_7 = \frac{qN_A}{N'^2}\left[\frac{(y_w|_{v=v_{\rm ds}}-a)}{\alpha}\exp\left[-\alpha(t-y_w|_{v=v_{\rm ds}})\right] - \frac{1}{\alpha^2}\exp\left[-\alpha(t-y_w|_{v=v_{\rm ds}})\right] - \left(\frac{y_w|_{v=0}-a}{\alpha}\right)\times\exp[-\alpha(t-y_w|_{v=0})] + \frac{1}{\alpha^2}\exp[-\alpha(t-y_w|_{v=v_{\rm ds}})]\right]$$

in which

$$\frac{1}{N'} = \frac{1}{N_A} + \frac{1}{N_{\rm dr}}.$$

Equation (34) is the expression for contribution to the total channel current due to the gate depletion region in which I_8 can be written as

$$I_8 = \frac{qN_{\rm dr}}{\varepsilon\alpha}\left[\left(y_{\rm dg}|_{v=v_{\rm ds}} - \frac{1}{\alpha}\right)\exp[-\alpha(t - y_{\rm dg}|_{v=v_{\rm ds}})] - \left(y_{\rm dg}|_{v=0} - \frac{1}{\alpha}\right)\exp[-\alpha(t - y_{\rm dg}|_{v=0})]\right]$$

The contribution to the total channel current by the carriers generated at the active layer-substrate interface depletion region is given by (35). I_9 and I_{10} of (35) are expressed as

$$I_9 = \frac{2}{\alpha}\left[\left(y_w|_{v=v_{\rm ds}} - \frac{1}{\alpha} - a\right)\exp[-\alpha(t - y_w|_{v=v_{\rm ds}})] - \left(y_w|_{v=0} - \frac{1}{\alpha} - a\right)\exp[-\alpha(t - y_w|_{v=0})]\right]$$

$$I_{10} = \frac{qN_{\rm dr}}{\varepsilon\alpha}\left[\left(y_{\rm ds}|_{v=v_{\rm ds}} - \frac{1}{\alpha}\right)\exp[-\alpha(t - y_{\rm ds}|_{v=v_{\rm ds}})] - \left(y_{\rm ds}|_{v=0} - \frac{1}{\alpha}\right)\exp[-\alpha(t - y_{\rm ds}|_{v=0})]\right].$$

REFERENCES

[1] C. Baack, G. Elze, and G. Walf, "GaAs MESFET: A high speed optical detector," *Electron. Lett.*, vol. 13, no. 7, p. 193, Mar. 1977.

[2] J. C. Gammel and J. M. Ballentyne, "The OPFET: A new high speed optical detector," in *Proc. IEDM*, 1978, pp. 120–123.

[3] H. Mizuno, "Microwave characteristics of an optically controlled GaAs MESFET," *IEEE Trans. Microwave Theory Tech.*, vol. MTT-31, pp. 596–600, July 1983.

[4] A. A. A. de Salles, "Optical control of GaAs MESFETs," *IEEE Trans. Microwave Theory Tech.*, vol. MTT-31, pp. 812–820, Oct. 1983.

[5] S. Mishra, V. K. Singh, and B. B. Pal, "The effect of surface recombination on the frequency dependent characteristics of an ion-implanted GaAs OPFET," *IEEE Trans. Electron Devices*, vol. 37, pp. 942–946, Apr. 1990.

[6] Y. Zebda and S. Abu Helweh, "AC Characteristics of optically controlled MESFET (OPFET)," *J. Lightwave Technol.*, vol. 15, pp. 1205–1211, July 1997.

[7] G. W. Taylor, H. M. Darley, and P. K. Chatterjee, "A device model for an ion-implanted MESFET," *IEEE Trans. Electron Devices*, vol. ED-26, pp. 172–182, Mar. 1979.

[8] S. M. Sze, *Physics of Semiconductor Devices*, 2nd ed. New Delhi, India: Wiley Eastern Ltd., 1983, p. 755.

[9] M. Shur, *GaAs Devices and Circuits*. New York: Plenum, 1987, pp. 309–322.

[10] B. B. Pal, Shubha, K. H. Kumar, and R. U. Khan, "Frequency dependent behavior of an ion-implanted GaAs OPFET considering photovoltaic effect and the gate depletion width modulation," *Solid State Electron.*, vol. 38, no. 5, pp. 1097–1102, 1995.

[11] Shubha, B. B. Pal, and R. U. Khan, "Optically controlled ion-implanted GaAs MESFET characteristic with opaque gate," *IEEE Trans. Electron Devices*, vol. 45, pp. 78–84, Jan. 1998.

[12] B. B. Pal and S. N. Chattopadhyay, "GaAs OPFET characteristics considering the effect of gate depletion modulation due to incident radiation," *IEEE Trans. Electron Devices*, vol. 39, pp. 1021–1027, May 1992.

Nandita Saha Roy received the B.Sc. and M.Sc. degrees in physics from Banaras Hindu University, Varanasi, India, in 1993 and 1995, respectively. Presently, she is working toward the Ph.D. degree on high-speed devices.

In September 1995, she joined the Department of Electronics Engineering, Institute of Technology, Banaras Hindu University as a Research Scholar.

B. B. Pal is a Professor at the Centre of Advanced Study, Department of Electronics Engineering, Institute of Technology, Banaras Hindu University, Varanasi, India.